VIA MEDICA

ORIGINAL PAPER / OBSTETRICS

Ginekologia Polska
2024, vol. 95, no. 9, 677–686

ISSN 0017–0011, e-ISSN 2543–6767

DOI: 10.5603/gpl.97942

# The discrepancy distribution of macrophage subsets in preeclampsia placenta with or without fetal growth restriction from a small cohort

**Wenhui Song[1*], Fengjiao Wang[1*], Xia Li[1*], Fangfang Liu[1], Tianxiao Yu[1], Xizhenzi Fan[1], Mingwei Li[1], Qing Guo[1, 2]**

*[1]The Fourth Hospital of Shijiazhuang, China*
*[2]Hebei Key Laboratory of Maternal and Fetal Medicine, China*
**Co-first authors*

## ABSTRACT

**Objectives:** To identify the effect of distribution characteristic of macrophages on placental function and angiogenesis in pregnancies with preeclampsia (PE) in presence of fetal growth restriction (FGR) or preeclampsia without FGR.

**Material and methods:** The study tested the hypothesis that there was association between distribution characteristic of macrophage subsets (marked by CD68, CD163, respectively) and placental capillary development, leading to placental dysfunction in PE pregnancies with FGR (n = 36). Changes in placental parameters related with efficiency and angiogenesis and macrophage phenotypes (CD68 and CD163) were evaluated by immunohistochemistry. Pearson correlation analysis was performed to analysis the association between macrophage phenotype and placental function as well the CD34 staining, respectively. Additionally, the localization of CD68 and CD163 was assessed by using immunoflurorescence staining.

**Results:** Pearson correlation analysis had shown the positive association between CD68 expression and microvessel formation and the reverse linear relationship between CD163 staining and placental sufficiency in PE + FGR placenta. The co-localization of CD163 and CD34 may pointed to the compensatory role of CD163 distribution involved in prompting neovascularization.

**Conclusions:** The association between disturbed distribution of macrophages and placental efficiency and angiogenesis were only found in PE with FGR not in PE pregnancies without FGR, underlying the discrepancy role of macrophage subsets depending on the clinical phenotype of PE pregnancies.

**Keywords:** preeclampsia; macrophage; fetal growth restriction; angiogenesis; placenta

Ginekologia Polska 2024; 95, 9: 677–686

## INTRODUCTION

Preeclampsia is a placental origin complication [1] characterized by insufficient placentation [2], endothelial dysfunction [3], inflammation and disturbed immune system [4]. The severity of preeclampsia was reported correlated with the placental insufficiency induced via unbalanced inflammatory status [5]. One of the common clinical manifestation in relation with severe preeclampsia is fetal growth restriction (FGR) [6]. The maintenance of normal placenta function plays an vital role in fetal development with sufficient nutrition and oxygen supply, possibly relying on the adaptation and plasticity of placental angiogenesis as well the response of immune cells to the insults [7, 8]. However, there existed contradictory manifestations on microvessel development in preeclampsia (PE) with and without FGR placentas [9, 10].

Placental macrophages mainly consist of macrophages distributed among fetal chorionic villus stromal exhibiting phenotypic and functional heterogeneity and plasticity. The heterogeneous population are involved in placental angiogenesis and hematopoiesis [11]. Two main subsets classified the macrophages: pro-inflammatory M1 type (CD68) and anti-inflammatory M2 type (CD163) [12]. M1 type (CD68) macrophages are involved in inflammatory process, while M2 type (CD163) macrophages serves as the key player of tissue remodeling and angiogenesis. M2 like macrophage distributed in the villous stroma, mostly close to feto-placental microvessels [12]. Since it has been shown the imbal-

**Corresponding author:**
Qing Guo
The Fourth Hospital of Shijiazhuang, China
e-mail: 45380023@qq.com

Received: 24.10.2023 Accepted: 1.01.2024 Early publication date: 31.01.2024

**Table 1. Demographic characteristic of study population**

| | PE + IUGR (n = 13) | PE (n = 13) | Control (n = 13) | p value |
|---|---|---|---|---|
| Maternal age [years] | 29.23 ± 3.17 | 29.00 ± 3.74 | 27.23 ± 3.56 | 0.29 |
| Weight [kg] | 62.00 ± 10.92 | 64.08 ± 12.64 | 54.77 ± 6.07 | 0.07 |
| Weight gain [kg] | 15.85 ± 6.09 | 18.32 ± 8.89 | 16.69 ± 5.07 | 0.65 |
| BMI [kg/m$^2$] | 24.27 ± 4.29 | 24.45 ± 4.29 | 21.41 ± 2.42 | 0.084 |
| Gravida ≥ 3 (n, %) | 4 (30.77) | 2 (15.38) | 1 (7.69) | 0.453 |
| Primiparous (n, %) | 6 (46.15) | 8 (61.54) | 13 (100) | 0.333 |
| Gestational at delivery [weeks] | 34.88 ± 2.67 | 35.46 ± 2.84 | 35.26 ± 2.78 | 0.86 |
| Systolic blood pressure [mmHg] | 143.73 ± 8.93$^{*}$ | 146.73 ± 12.03$^{*}$ | 114.54 ± 8.32$^{+\#}$ | < 0.001 |
| Diastolic pressure [mmHg] | 93.94 ± 7.02$^{*}$ | 92.00 ± 8.09$^{*}$ | 76.00 ± 8.10$^{+\#}$ | < 0.001 |
| Gestational diabetes (n, %) | 1 (7.69) | 6 (46.15)* | 0 (0.00)$^{+}$ | 0.009 |
| Hypothyroidism (n, %) | 4 (30.77) | 3 (23.08) | 0 (0.00) | 0.128 |
| IVF-ET (n, %) | 0 (0.00) | 1 (7.69) | 0 (0.00) | 1.000 |
| Fetal birth weight [g] | 1875.38 ± 439.99$^{*+}$ | 2582.31 ± 372.25$^{*\#}$ | 3232.31 ± 290.75$^{+\#}$ | < 0.001 |
| Fetal gender (male) (n, %) | 6 (46.15) | 8 (61.54) | 8 (61.54) | 0.777 |
| Fetal gender (female) (n, %) | 7 (53.85) | 5 (38.46) | 5 (38.46) | – |

Data are presented as mean ± standard deviation or number (percentage); PE — preeclampsia; FGR — fetal growth restriction; BMI — body mass index; IVF-ET — *in vitro* fertilization and embryo transfer. Statistical significance: *p < 0.05 vs normotensive; $^{+}$p < 0.05 vs PE without FGR; $^{\#}$p < 0.05 vs PE with FGR

ance between the M1/M2 macrophage in the placenta is observed during pregnancy with fetal growth retardation, as well as in PE [13, 14]. However, the discrepancy distribution of M1 and M2 macrophages on placental efficiency and associated angiogenesis of placenta from pregnancies with both PE and FGR are still warranted to be further explored.

The aim of our study was to identify the effect of distribution characteristic of macrophages on placental efficiency and microvessel formation of placenta in pregnancies with PE and PE with FGR. However, when stratifying by only PE and PE with FGR, we hypothesized that there also could be a relationship between the distribution of macrophages with capillary adaptation, mainly leading to the disturbed placental efficiency, especially in PE pregnancies with FGR.

## MATERIAL AND METHODS

### Human subjects

Human subjects were recruited following written informed consent and studies performed following the approval of the local ethics committee (Approval ID: 20210030). The inclusion for this study were singleton placentas from gestational age matched normotensive and PE pregnancies collected from the Fourth Hospital of Shijiazhuang. Based on fetal birth weight, PE pregnancies were clarified into PE in presence with FGR and without FGR. In total, they were classified into three groups: normotensive group, PE group, and PE + FGR group.

Preeclampsia was defined as an elevated blood pressure of ≥ 140/90 mmHg (on no less than 2 occasions at least 6 hours apart) that appeared after 20$^{th}$ gestation week in a previous normotensive woman and accompanied by proteinuria containing no less than 0.3 g in 24 hours [15]. The FGR was defined as fetal weight less than the 10$^{th}$ percentile for gestation age companying with the failure to reach its genetically growth potential [16]. Criteria for exclusion included twins or multiple birth, congenital malformation, severe placental calcification or infarction, and umbilical cord compromise. The demographic characteristic and pregnancy outcomes were collected and detailed in Table 1.

### Placenta collection

Placenta sample was collected immediately after the delivery. And then, placental weight and size were recorded after fetal membranes and the umbilical cord were removed. Placental efficiency and placental volume (cm$^3$) were calculated and recorded [17]. A portion of feto-placenta fragments was collected and fixed overnight at 4°C in 4% paraformaldehyde and embedded in paraffin for immunohistochemical and immunofluorescence analysis.

### Real-time reverse transcriptase-polymerase chain reaction (RT-PCR)

Frozen placental tissue (80–100mg) was homogenized using tissue cryogrinder (KZ-III-FP, Wuhan Servicebio Technology Company Limited, CH) and total RNA was extracted with Eastep@Supper Total RNA Extraction kit (Shanghai Promega Biological Products Ltd., Shanghai, CH) following manufacture's recommendation. And then, 1000 ng

of total RNA was reverse transcribed to complementary DNA (cDNA) with first-strand complementary synthesis system (Invitrogen, Life Technologies). The relative mRNA expression was assessed following the instruction of PowerUp SYBR Green Master Mix (ThermoFisher) and normalized to the endogenous reference gene GAPDH using the ΔΔCT method. The primers used were listed as follows: CD68 forward primer: 3′-GCTACATGG CGGTGGAGTACAA-5′, reverse primer: 3′-ATGATGAGAGGC AGC AAGATGG-5′; CD 163 forward primer: 3′-CAACTTGAGTCCCTTCACCA-5′, reverse primer: 3′-CCACTCC TCCTGGACTTTCA-5′.GAPDH forward primer: 3′-GGAAGCTTGTCATCAATGGAAA TC-5′, reverse primer: 3′-TGATGACCCTTTTGGCTCCC-5′.

### Automated immunohistological staining and digital analysis

Paraffin embedded formalin-fixed human placenta tissue was sectioned (4 microns) and processed for immunostaining with a mouse monoclonal anti-human CD34 primary antibody (QBEnd 10, Gene Tech, Shanghai, CH) and CD68 (KPI, Gene Tech, Shanghai, CH) diluted with ratio of 1:200, and CD163 (Proteintech, Wuhan, CH) immunostaining with 1:2000 dilution as vendor's recommendation, respectively. The immunostaining process was automated performed with UltraView Universal DAB Detection Kit (Ventana Medical System, Tucson, AZ USA) on VENTANA BenchMark GX@ (Roche, Tucson, AZ USA) staining instrument following manufacturer recommended protocol. Digital scan of stained slides was performed at 20× magnification using Aperio CS2 Digital Pathology Scanner (Aperio Technologies Inc. San Diego USA). For each slide, five equal size regions of interest [(ROI) 0.2645 $\mu m^2$ each] were selected by experienced pathologist. Regions of interest was restricted to the microvessel rich area from different locations. All the analysis associated with staining intensity was performed by using Aperio Imagescope software (Aperio Technologies Inc. San Diego USA) [18]. To calculate CD34 staining in placenta, color deconvolution and microvessel analysis algorithms were employed to quantify microvessel density associated parameters, respectively. Similarly, the membrane color deconvolution was used for CD68 (KPI, Gene Tech, Shanghai, CH) and CD163 (Proteintech, Wuhan, CH) staining analysis. The threshold for color saturation was set using positive and negative control tissues and adjusted it by testing the randomly selected placenta tissue accordingly. Algorithm parameters were translated into negatively (blue), moderately (orange) and strongly (red) stained manifestation. Raw data was presented as number of positive pixels and staining intensity of positive pixels which was normalized to total positive pixels counts or field of ROI region in $\mu m^2$. To evaluate the accuracy of digital qualification, immunohistochemistry (IHC) slides were inspected by an experienced pathologist, using a scoring system from 0 to 3 to differentiate staining intensity.

### Dual-labelling Immunofluorescence analysis

Localization of markers of macrophage subset (CD68, CD163) with CD34 was assessed followed the procedure as previously described [19, 20]. Frozen placental sections were used for dual-labelling immunofluorescence. Optimal cutting temperature compound (OCT) embedded frozen human placenta tissue was cut into 8μm-thick-section. After OCT was removed, antigen retrieval and blockage (3% $H_2O_2$ and 5% bovine serum albumin [BSA]) was performed. Then the placental sections were incubated with primary antibodies overnight at 4°C: CD34 (Mouse, 60180-1-Ig, Proteintech, China) with CD68 (Rabbit, 1:200, 28058-1-AP, Proteintech, China) or CD163 (Rabbit, 1:200, 16646-1-AP, Proteintech, China) for double immunolabeling procedure. And then the goat anti-mouse IgG (DyLight 488, A23210) (Abbkine Scientific Co.,Ltd, Wuhan, China) was used as the secondary antibody for CD34 and goat anti-rabbit IgG (DyLight 649, A23620) (Abbkine Scientific Co.,Ltd, Wuhan, China) for CD68 and CD163 at room temperature for 1 h. Then the nucleus was counterstained with 4 , 6 - diamidino-2-phenylindole (DAPI) stain solution. Finally, a FV3000 confocal laser scanning microscope (Olympus) was employed to observe and capture images.

### Statistical analysis

Data were presented as mean ± SD or number of frequency (percentage). The One-way ANOVA and Student T test were used for variate analysis. Fisher's exact test was employed for univariate analysis. Data analysis was performed using SPSS version 24.0 and the statistical plots were created using GraphPad Prism 8.0 software. Pearson's correlation analysis was carried out to identify the correlation between placental function and microvessel parameter and other univariates. P value less than 0.05 was considered significant.

## RESULTS

### Clinical characteristics and laboratory parameters of the study population

A summary of demographic characteristics and laboratory indexes were listed in Table 1 and 2. As shown in Table 1, the blood pressure was elevated significantly in two PE groups compared with control group, respectively ($p < 0.05$). The incidence of gestational diabetes was significantly different between the three groups. However, no significant difference was evident between the three groups with respect to age, body mass index and delivered gestational age.

With respected to the fetal birth weight, it was significantly lower in PE + FGR and PE group compared with normotensive pregnant group ($p < 0.001$). Notably, the

**Table 2.** The maternal laboratory indexes of preeclampsia (PE) + intrauterine growth retardation (IUGR), PE and control group

| | PE + IUGR (n = 13) | PE (n = 13) | Control (n = 13) | p value |
|---|---|---|---|---|
| WBC count | 8.63 ± 1.70 | 8.62 ± 1.27 | 10.07 ± 4.73 | 0.489 |
| Neutrophils count | 6.29 ± 1.81 | 6.42 ± 1.26 | 7.89 ± 4.52 | 0.233 |
| Neutrophil percent | 71.76 ± 8.89 | 73.99 ± 4.81 | 78.67 ± 6.89 | 0.051 |
| Lymphocyte count | 1.88 ± 0.47* | 1.72 ± 0.26 | 1.66 ± 0.56# | 0.017 |
| Lymphocyte percent | 22.75 ± 7.63* | 20.40 ± 4.54 | 15.72 ± 5.91# | 0.020 |
| Monocyte count | 0.39 ± 0.14 | 0.40 ± 0.11 | 0.46 ± 0.17 | 0.428 |
| Monocyte percent | 4.73 ± 1.81 | 4.72 ± 1.11 | 4.96 ± 1.50 | 0.896 |
| Hemoglobin | 117.85 ± 13.28 | 116.77 ± 7.90 | 119.00 ± 12.92 | 0.888 |
| Platelet | 184.85 ± 63.41 | 170.54 ± 37.68 | 192.15 ± 46.27 | 0.543 |
| D-dimer | 415.77 ± 230.08* | 469.46 ± 204.88 | 770.62 ± 488.80# | 0.022 |
| Fibrinogen | 3.36 ± 0.59* | 3.15 ± 1.28 | 4.21 ± 0.58# | 0.015 |
| ALT | 14.14 ± 7.20 | 12.62 ± 6.76 | 11.62 ± 5.35 | 0.594 |
| AST | 21.15 ± 8.18 | 18.00 ± 3.21 | 18.23 ± 5.14 | 0.321 |
| TBA | 4.47 ± 2.95 | 3.492.49 | 3.381.73 | 0.464 |
| Cr | 54.6112.21 | 54.0515.76 | 51.1012.29 | 0.778 |
| BUN | 394.62 ± 68.34* | 405.46 ± 94.99* | 258.31 ± 63.12+# | < 0.001 |

Data are presented as mean ± standard deviation or number (percentage); WBC — white blood cell; ALT — glutamic pyruvic transaminase; AST — glutamic oxaloacetic transaminase; TBA — total bile acid; Cr — creatinine; BUN — blood urea nitrogen. Statistical significance: *p < 0.05 vs normotensive; +p < 0.05 vs PE without FGR; #p < 0.05 vs PE with FGR

significant difference was observed between PE + FGR and PE group (p < 0.05). As shown in Table 2, the quantity and percentage of lymphocyte in plasma from pregnant women was significant higher in PE with FGR group compared with normotensive pregnant group (p = 0.017, p = 0.020). With respected to the coagulation-related factors, the concentration of fibrinogen in maternal plasma was observed significantly lower only in preeclampsia with FGR group compared with control group (p = 0.015). Likewise, the concentration of D-dimer was shown elevated in plasma from preeclampsia women with FGR and without FGR compared with normotensive pregnant women (p = 0.022). On the other hand, there was the significant increase in plasma concentration of blood urea nitrogen (BUN) in two preeclampsia groups compared with normotensive pregnant group (p < 0.001). However, no significant difference was evident in other parameters between different groups.

### Compromised microvessel formation and polarized macrophage distribution may contribute to placental dysfunction among PE with FGR and PE group

The placental characteristics comparing the PE + FGR, PE and control group were shown in Table 3. A significant lowered placental weight was revealed in PE + FGR group compared with PE group (p < 0.05). Likewise, the placental efficiency calculated as the ratio of birth weight to the placental weight showed significantly lower in PE with FGR individuals compared with PE mothers. Similarly, there was a trend towards reduction in the placenta volume in the two PE groups however this did not reach significance.

Furthermore, to evaluate the capillary formation, endothelial marker CD34 expression was assessed. It was shown the significant reduced strong CD34 staining in PE groups compared with control group (p < 0.001). Similarly, the total positive percentage of CD34 was revealed a significant decrease accompany with the significant reduced capillary density in PE complicated with FGR pregnancies compared with control group (p < 0.05).

To detect the distribution and number of macrophages in placenta tissue, relative gene expression (Fig. 1) and immunohistochemistry analysis of CD68 and CD163 were performed as respective marker of M1 and M2 characterized macrophage (Fig. 2). The gene relative expression of CD163 was significantly lower among the placentas from PE + FGR group compared with control group (p = 0.03), while the same trend was not found between PE and control group (p > 0.05). However, no change was found in CD68 relative gene expression among groups (p > 0.05). Macrophage positive for CD68 and CD163 were both found localized adjacent to capillary in villous stroma. Based on the pixel quantification, the total positive percentage of CD68 revealed a significantly increased in PE with FGR group compared with PE group (p < 0.05), along with the significantly increased number of the subset of macrophage. In contrast,

**Table 3. Placenta associated parameters and CD34, CD68, CD163 IHC staining analysis**

| | PE + IUGR (n = 13) | PE (n = 13) | Control (n = 13) | p value |
|---|---|---|---|---|
| Placental weight [g] | 394.23 ± 81.98$^{+}$ | 487.69 ± 94.84$^{\#}$ | 464.62 ± 95.29 | 0.034 |
| Placental volume [cm$^3$] | 582.73 ± 131.64 | 598.31 ± 167.83 | 711.31 ± 213.75 | 0.136 |
| Placental efficiency [ratio] | 4.93 ± 1.60$^{*}$ | 5.44 ± 1.14$^{*}$ | 7.16 ± 1.21$^{+\#}$ | < 0.001 |
| CD34 percent total positive [%] | 66.96 ± 10.31$^{*}$ | 70.54 ± 13.73 | 81.92 ± 9.50$^{\#}$ | 0.005 |
| CD34 percent strong positive [%] | 8.89 ± 4.88$^{*}$ | 8.56 ± 5.29$^{*}$ | 19.64 ± 4.40$^{+\#}$ | < 0.001 |
| CD34 microvessel density | 2.47 ± 0.92$^{*}$ | 3.39 ± 1.22 | 4.43 ± 2.31$^{\#}$ | 0.015 |
| CD68 positive cells | 7458.08 ± 2458.75$^{+}$ | 5049.23 ± 2427.91$^{\#}$ | 5874.69 ± 1737.37 | 0.029 |
| CD68 percent total positive [%] | 87.75 ± 6.72$^{+}$ | 75.86 ± 14.56$^{\#}$ | 81.37 ± 8.43 | 0.023 |
| CD163 positive cells | 5490.00 ± 2411.24 | 5852.62 ± 2269.52 | 6040.85 ± 1796.28 | 0.807 |
| CD163 percent total positive [%] | 62.75 ± 15.66$^{*}$ | 73.65 ± 19.14 | 83.27 ± 16.53$^{\#}$ | 0.016 |

Data are presented as mean ± standard deviation or number (percentage); PE — preeclampsia; IUGR — intrauterine growth retardation. Statistical significance: *p < 0.05 vs normotensive; $^{+}$p < 0.05 vs PE without FGR; $^{\#}$p < 0.05 vs PE with FGR

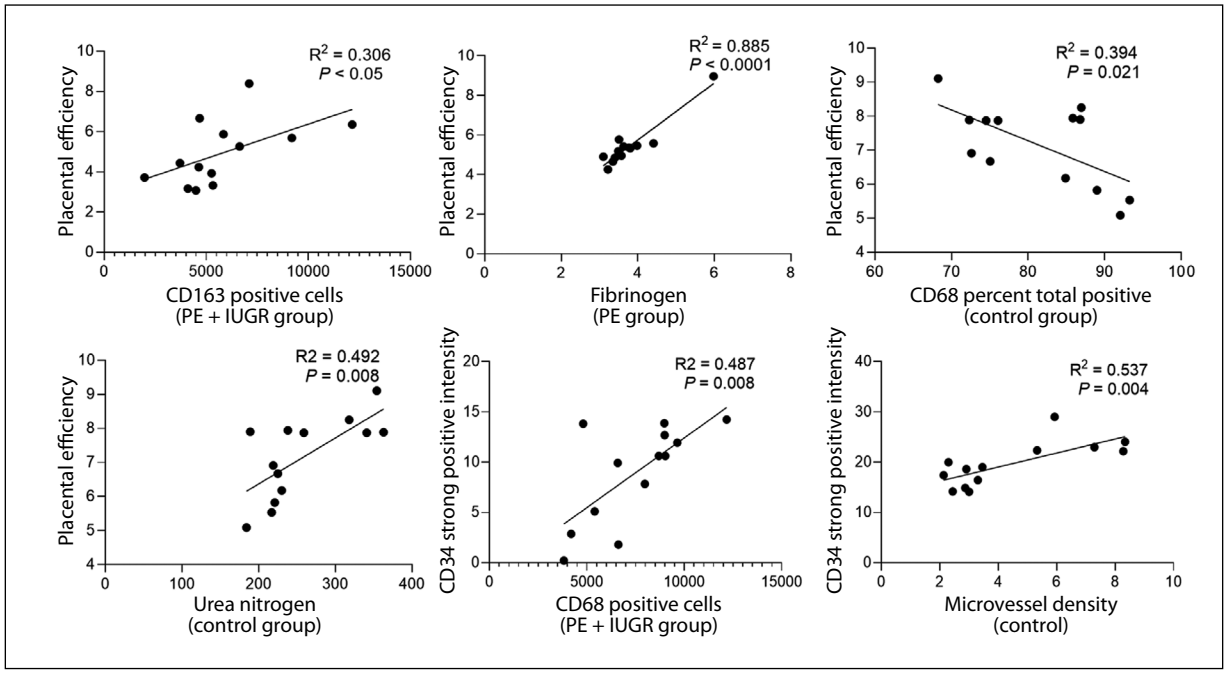


**Figure 1.** Association between multivariate and placental function and capillary formation stratified by groups; PE — preeclampsia; IUGR — intrauterine growth retardation

pixel quantification revealed a significantly decreased total staining frequency of CD163 in PE group complicated with FGR, manifesting a trend of reduced number of M2 characterized macrophage in the related group.

## Association between multi-variates and placental function and capillary formation in groups

The correlations between multi-variates and placental efficiency as well as capillary formation manifested with CD34 strong positive intensity are shown in Figure 3 stratified by different groups. A positive correlation between quantity of CD163 positive cell and placental efficiency was detected only in PE + FGR group ($R^2$ = 0.306; p < 0.05). In contrast, there was an inverse correlation shown between total positive percentage of CD68 and placental efficiency in control group ($R^2$ = 0.394; p = 0.021). With respect to laboratory parameters, there was a statistical correlation towards an increased fibrinogen concentration in maternal plasma and an improved placental efficiency manifested in PE group ($R^2$ = 0.885; p < 0.0001). While the higher concentration of urea nitrogen in peripheral blood was positively corre-

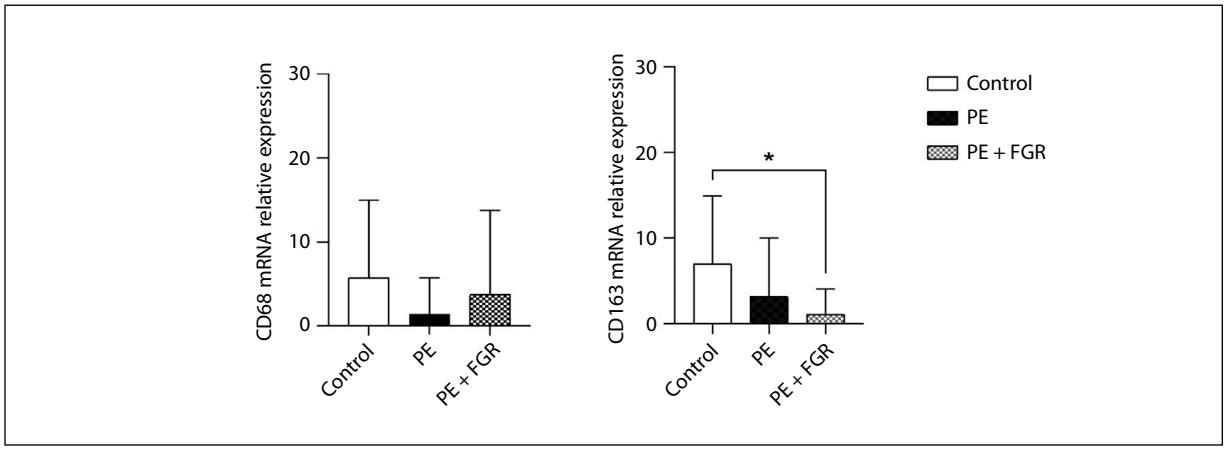


**Figure 2.** The gene expression of CD163 and CD68 in placentas from preeclampsia (PE), PE + fetal growth restriction (FGR) and control pregnancies. Data are presented as mean ± standard error of mean (SEM). Asterisk (*) represents $p < 0.05$ by Student's t-test

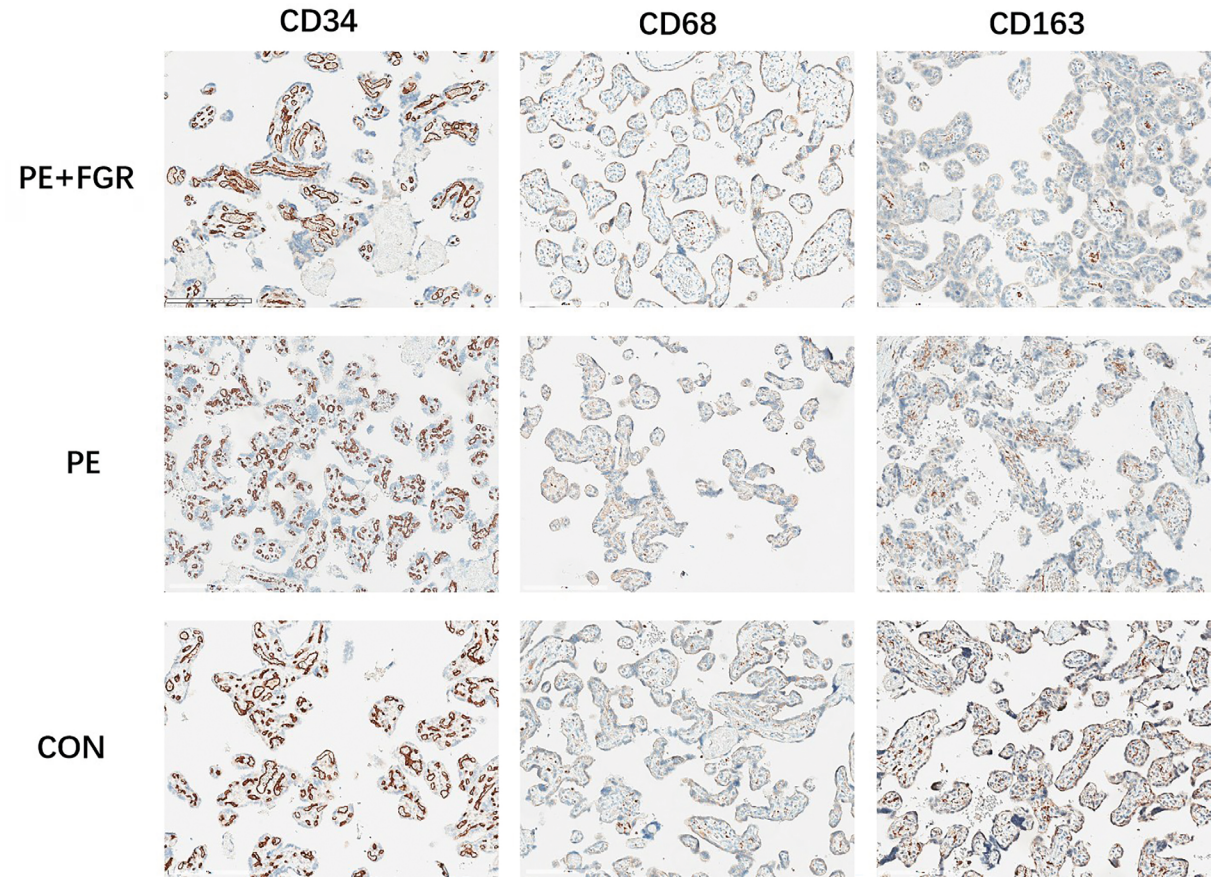


**Figure 3.** Immunohistochemistry staining of CD34, CD68 and CD163 in placenta tissue (magnification). The size of scale bar is 200 µm, marked at the left foot corner of each image; PE — preeclampsia; FGR — fetal growth restriction; CON — control

lated with placental efficiency in control group ($R^2 = 0.492$; $p = 0.008$), no correlation was noted between placental function vs other variates in normotensive pregnant women. With respected to microvessel formation, the positive linear relationship was observed between CD34 strong positive staining intensity and microvessel density in control group ($R^2 = 0.537$; $p = 0.004$), however, the increased staining of CD34 was significantly correlated with the raised amount of $CD68^+$ macrophage only in PE + FGR group ($R^2 = 0.487$; $p = 0.008$).

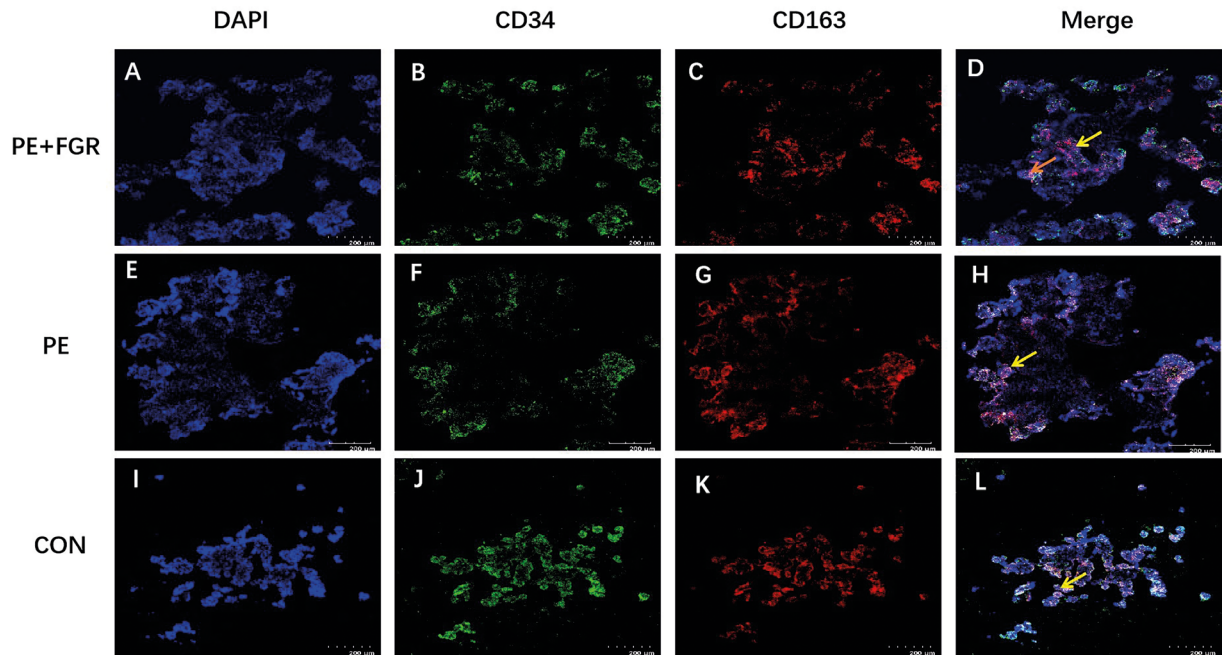


**Figure 4.** Dual Immunofluorescence staining of CD34 and CD163 in fetoplacental tissue (40× magnifcation). **A. E. I.** Nuclei was stained with DAPI (blue) in PE+FGR, PE, Control group, respectively; **B. F. J.** CD34 positive expression was stained in green in PE+FGR, PE, Control group, respectively; **C. G. K.** CD163 expression in microvilli was stained in red in PE+FGR, PE, Control group, respectively; **D.** The two characteristics of colocalization of CD34 and CD163 were found in preeclampsia (PE) + fetal growth restriction (FGR) placenta as follows, colocalizationin villous stroma (yellow arrow) and at the edge of microvillous adjacent to syncytiotrophoblast (orange arrow); **H.** Colocalization of CD34 and CD163 adjacent to the syncytiotrophoblast was found in PE placenta marked with yellow arrow; **L.** CD34 and CD163 coimmunostaining distributed as an outline of microvillous (yellow arrow) similarly with (H) manifestation. The size of scale bar is 200 μm; CON — control

### Exclusive distributed features of CD68 and CD163 based on the clinical manifestation of preeclampsia

The double staining was performed by using immunofluorescence (IF) to identify the localization features of CD163 and CD68 with CD34, respectively (Fig. 4 and 5). As shown in Figure 4, in PE + FGR placenta, the colocalization of CD34 and CD163 was observed. Furthermore, two characteristics of colocalization were revealed under confocal microscopy observation, displayed as distributed adhere to the syncytiotrophoblast and among the villous stroma. However, the distribution adjacent to syncytiotrophoblast was exhibited both in PE and control group. The findings on CD68 staining also showed the specific distribution traits among the three groups. Inconsistently with CD163 IF staining, CD68 staining was predominantly distributed at the edge of microvillous in placenta from PE + FGR pregnancies, accompany with scattered expression in the stroma. The colocalization of CD68 and CD34 was shown mainly among the stroma in PE group, while CD68 localization was similar with CD163 distribution in placenta tissue from control placental samples (Fig. 5).

## DISCUSSION

The balance of M1 and M2 participated in the regulation of pregnancy process [21]. Such disturbance may be involved in the development of complicated pregnancy, demonstrating its plasticity when it responds to the local insults [8]. Macrophages seem to be switched toward a pro-inflammatory (M1) phenotype in women with preeclampsia [22]. Thus, the pathophysiology of preeclampsia may be related with disturbed proportion of M1 and M2 macrophages.

It was suggested that the CD163, representative of M2 type macrophage, was downregulated in PE placental tissue compared with normotensive pregnancies [23]. Notably, it was revealed that the significantly reduced expression of CD163 in PE pregnancies complicated with FGR, while the trend to decrease in CD163 expression in PE placenta. As consequence, the significantly reduced microvessel density only presented in PE pregnancies with FGR as reported [9]. On the other hand, the significant higher CD68 positive staining was observed in PE pregnancies in presence of FGR vs PE group without FGR, consistently with previous study [24]. Furthermore, the positive relationship between CD68 and CD34 strong staining was shown in PE + FGR placenta. M1 macrophage acquires the capability of secretion pro-inflammatory cytokines, including IL-1β, IL-6 and TNFα. To our knowledge, IL-1β was reported the regulator of facilitating M2 macrophage infiltration and angiogenesis [25] responsible for the relationship between CD68 and CD34 staining. Similarly, the higher CD163/CD68 ratio was

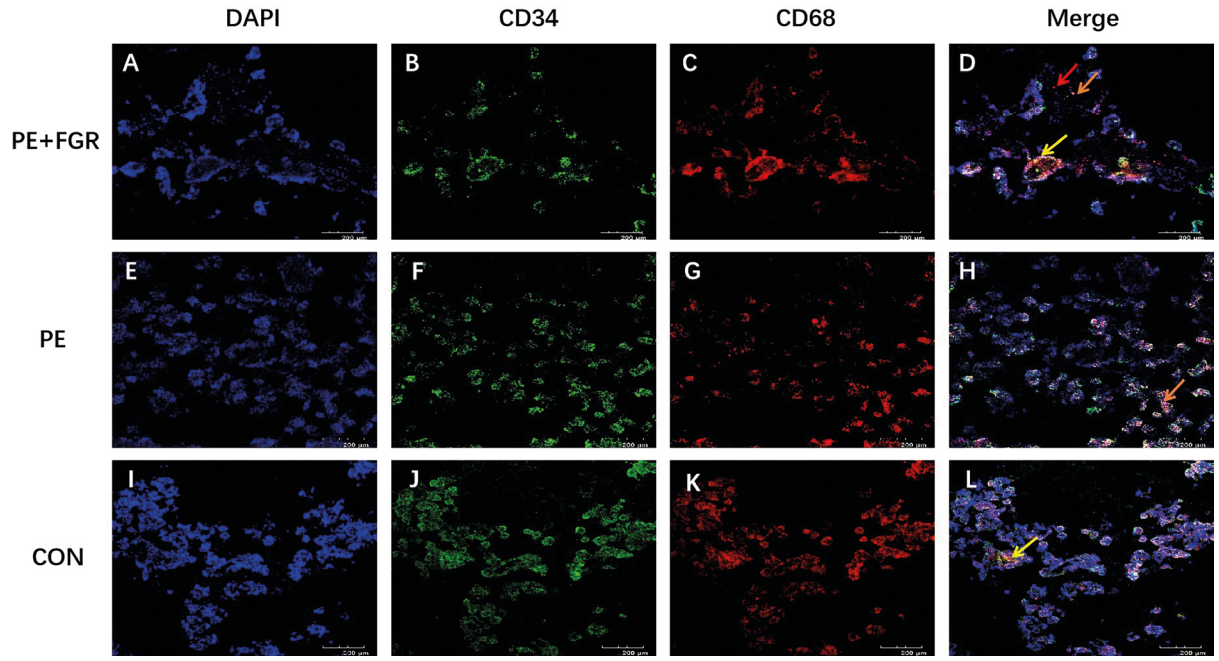


**Figure 5.** Dual Immunofluorescence staining of CD34 and CD68 in fetoplacental tissue section (40-fold magnifcation). **A. E. I.** Nuclei were stained with DAPI (blue) in PE+FGR, PE, Control group, respectively; **B. F. J.** CD34 positive expression was stained in green in PE+FGR, PE, Control group, respectively; **C. G. K.** CD68 expression in microvilli was stained in red in PE+FGR, PE, Control group, respectively; **D.** Two distribution features of co-expression were manifested in preeclampsia (PE) + fetal growth restriction (FGR) fetoplacental, in villous stroma (yellow arrow) and adjacent to syncytiotrophoblasts (orange arrow). Also, the scattered CD163 distribution among the stroma was also observed (rea arrow); **H.** The colocalized staining of CD68 and CD34 in stroma was outstand with yellow arrow; **L.** Immunofluorescence (IF) staining of CD68 and CD34 adhere to syncytiotrophoblast was present (orange arrowhead). Scale bar is 200 μm; CON — control

reported in FGR placentas that may aggravates placental insufficiency and fetal growth[26]. The characteristic of macrophage infiltration may suggest a similar trend towards activated macrophage function [27]. In contrast, the reverse association was suggested between placental function and CD68 expression in control group reported involved in the development of the normal feto-placenta [28].

In our study, it was shown that the compromised placental insufficiency in line with the decreased microvessel density in two PE groups, especially the PE pregnancies complicated with FGR. Placental efficiency was positively associated with the expression of CD163, suggesting the compensatory role of M2 like macrophage responding to the local insults on maintaining placental competence in group of PE + FGR. Thus, it was suggested the fact that the local insults as the trigger of macrophage polarization may be more abundant in placenta from PE with FGR pregnancies than group of PE without FGR. However, in PE group, there was no observed association between CD68 and CD163 and placental function. The placental sufficiency was positively correlated with serum level of maternal fibrinogen. Conclusively, the evidence may underlie the deviated macrophage role depending on the clinical manifestation of PE pregnancies.

Furthermore, the double staining of immunofluorescence was employed to evaluate the localization characteristic of macrophage subsets. To our knowledge, this is the preliminary study to show the evidence of colocalization of CD163 and CD34 in placenta from pregnancies of PE with FGR, while the co-expression of CD68 and CD34 in PE group, probably underlying the effect of both two subsets on microvessel development dependent on specific local insult. It was reported that macrophage polarization towards an M2 phenotype had a higher pro-angiogenic potential [29], indicating the contributing role on the adapted changes of placental function [30]. As well, pro-inflammatory cytokines secreted by M1 macrophage acted as candidates involved in the process of angiogenesis [25]. Not only co-staining with CD34, but it was also observed the immunostaining of CD163 was adjacent to syncytiotrophoblast, which was potentially involved in regulating the phenotype transition of macrophage and existed two-way adjusting effect on CD163 and CD68 [31].

However, further investigation was required to explore the mechanism for switching phenotype of macrophage.

## CONCLUSIONS

Taken together, placental resident macrophages exhibited the different infiltration pattern relying on the clinical performance of PE (in presence of FGR or not), indicative of severe compromised placental function and decrease capillary quantity in PE + FGR placenta.

### Strength and limitations

The study provides evidence for the involvement of placental resident macrophages in the process of regulating placental efficiency and angiogenesis in PE pregnancies. Importantly, our preliminary observation suggested the different distributed pattern of macrophages among PE with FGR, without FGR and normotensive pregnancies. However, as this study was conducted in a small set of recruitments, the larger size of participants was needed to verify the findings. Also, the molecule mechanism was remained to be further explored.

## Article information and declarations

### *Data availability statement*

The data supporting our findings are available on request from the corresponding author. Due to the privacy of patients and legal restrictions, the data are not available publicly.

### *Ethics statement*

All participants signed informed consent and the procedure conduced in coincidence with the Declaration of Helsinki. The local approval was supported by the Ethics Committee of The Fourth Hospital of Shijiazhuang (Approval ID: 20210030).

### *Author contributions*

Song W wrote the original draft, preformed the experiment and applied the funding.

Wang F collected data and samples, performed part of the experiment.

Li X contributed to data collection and funding application.

Liu F conducted the quality control of placental samples and data summary.

Yu T contributed to manuscript revision preliminarily.

Fan X contributed to design the experiment.

Li M contributed to the statistical analysis.

Guo Q supervised the process of the project and made considerable revision on the original MS. All authors approved the final version of manuscript.

### *Funding*

This investigation was supported by Health Commission of Hebei Province (NO.20181065) and Hebei Provincial Department of Human Resources and Social Security (NO. C20200358). As well, the funding from the Natural Science Foundation of Hebei Province (NO.H2021106030) was received.

### *Acknowledgements*

This study is supported by grants from Natural Science Foundation of Hebei Province in China (No.H2021106030), Hebei Provincial Department of Human Resources and Social Security (NO.C20200358) and Health Commission of Hebei Province (NO. 20181065).

### *Conflict of interest*

All the authors declared that they have no relevant financial interest to disclose.

### *Supplementary material*

None.

## REFERENCES

1. Wu JL, Jia J, He MZ, et al. Placental Origins of Preeclampsia: Potential Therapeutic Targets. Curr Med Sci. 2019; 39(2): 190–195, doi: 10.1007/s11596-019-2018-2, indexed in Pubmed: 31016509.
2. Raguema N, Moustadraf S, Bertagnolli M. Immune and Apoptosis Mechanisms Regulating Placental Development and Vascularization in Preeclampsia. Front Physiol. 2020; 11: 98, doi: 10.3389/fphys.2020.00098, indexed in Pubmed: 32116801.
3. Sánchez-Aranguren LC, Prada CE, Riaño-Medina CE, et al. Endothelial dysfunction and preeclampsia: role of oxidative stress. Front Physiol. 2014; 5: 372, doi: 10.3389/fphys.2014.00372, indexed in Pubmed: 25346691.
4. Michalczyk M, Celewicz A, Celewicz M, et al. The Role of Inflammation in the Pathogenesis of Preeclampsia. Mediators Inflamm. 2020; 2020: 3864941, doi: 10.1155/2020/3864941, indexed in Pubmed: 33082708.
5. Aisagbonhi O, Morris GP. Human Leukocyte Antigens in Pregnancy and Preeclampsia. Front Genet. 2022; 13: 884275, doi: 10.3389/fgene.2022.884275, indexed in Pubmed: 35571013.
6. Laskowska M, Laskowska K, Oleszczuk J. Interleukin-18 concentrations in pregnancies complicated by preeclampsia with and without IUGR: A comparison with normotensive pregnant women with isolated IUGR and healthy pregnant women. Pregnancy Hypertens. 2011; 1(3-4): 206–212, doi: 10.1016/j.preghy.2011.07.003, indexed in Pubmed: 26009028.
7. Leavey K, Grynspan D, Cox BJ. Both „canonical" and „immunological" preeclampsia subtypes demonstrate changes in placental immune cell composition. Placenta. 2019; 83: 53–56, doi: 10.1016/j.placenta.2019.06.384, indexed in Pubmed: 31477208.
8. Brown MB, von Chamier M, Allam AB, et al. M1/M2 macrophage polarity in normal and complicated pregnancy. Front Immunol. 2014; 5: 606, doi: 10.3389/fimmu.2014.00606, indexed in Pubmed: 25505471.
9. Egbor M, Ansari T, Morris N, et al. Morphometric placental villous and vascular abnormalities in early- and late-onset pre-eclampsia with and without fetal growth restriction. BJOG. 2006; 113(5): 580–589, doi: 10.1111/j.1471-0528.2006.00882.x, indexed in Pubmed: 16579806.
10. Mayhew TM, Wijesekara J, Baker PN, et al. Morphometric evidence that villous development and fetoplacental angiogenesis are compromised by intrauterine growth restriction but not by pre-eclampsia. Placenta. 2004; 25(10): 829–833, doi: 10.1016/j.placenta.2004.04.011, indexed in Pubmed: 15451198.
11. Liang G, Zhou C, Jiang X, et al. De novo generation of macrophage from placenta-derived hemogenic endothelium. Dev Cell. 2021; 56(14): 2121–2133.e6, doi: 10.1016/j.devcel.2021.06.005, indexed in Pubmed: 34197725.
12. Loegl J, Hiden U, Nussbaumer E, et al. Hofbauer cells of M2a, M2b and M2c polarization may regulate feto-placental angiogenesis. Reproduction. 2016; 152(5): 447–455, doi: 10.1530/REP-16-0159, indexed in Pubmed: 27534571.
13. Durst JK, Tuuli MG, Stout MJ, et al. Degree of obesity at delivery and risk of preeclampsia with severe features. Am J Obstet Gynecol. 2016; 214(5): 651.e1–651.e5, doi: 10.1016/j.ajog.2015.11.024, indexed in Pubmed: 26640073.
14. Medeiros LTL, Peraçoli JC, Bannwart-Castro CF, et al. Monocytes from pregnant women with pre-eclampsia are polarized to a M1 phenotype. Am J Reprod Immunol. 2014; 72(1): 5–13, doi: 10.1111/aji.12222, indexed in Pubmed: 24689463.
15. Gestational Hypertension and Preeclampsia: ACOG Practice Bulletin Summary, Number 222. Obstet Gynecol. 2020; 135(6): 1492–1495, doi: 10.1097/AOG.0000000000003892, indexed in Pubmed: 32443077.

16. Vayssière C, Sentilhes L, Ego A, et al. Fetal growth restriction and intra-uterine growth restriction: guidelines for clinical practice from the French College of Gynaecologists and Obstetricians. Eur J Obstet Gynecol Reprod Biol. 2015; 193: 10–18, doi: 10.1016/j.ejogrb.2015.06.021, indexed in Pubmed: 26207980.
17. Marques MR, Grandi C, Nascente LM, et al. Placental morphometry in hypertensive disorders of pregnancy and its relationship with birth weight in a Latin American population. Pregnancy Hypertens. 2018; 13: 235–241, doi: 10.1016/j.preghy.2018.06.020, indexed in Pubmed: 30177058.
18. Kalra J, Dragowska WH, Bally MB. Using Pharmacokinetic Profiles and Digital Quantification of Stained Tissue Microarrays as a Medium-Throughput, Quantitative Method for Measuring the Kinetics of Early Signaling Changes Following Integrin-Linked Kinase Inhibition in an In Vivo Model of Cancer. J Histochem Cytochem. 2015; 63(9): 691–709, doi: 10.1369/0022155415587978, indexed in Pubmed: 25940338.
19. Mao Q, Chu S, Shapiro S, et al. Increased placental expression of angiotensin-converting enzyme 2, the receptor of SARS-CoV-2, associated with hypoxia in twin anemia-polycythemia sequence (TAPS). Placenta. 2021; 105: 7–13, doi: 10.1016/j.placenta.2021.01.008, indexed in Pubmed: 33497931.
20. Seo H, Bazer FW, Burghardt RC, et al. Immunohistochemical Examination of Trophoblast Syncytialization during Early Placentation in Sheep. Int J Mol Sci. 2019; 20(18), doi: 10.3390/ijms20184530, indexed in Pubmed: 31540219.
21. Erlebacher A. Immunology of the maternal-fetal interface. Annu Rev Immunol. 2013; 31: 387–411, doi: 10.1146/annurev-immunol-032712-100003, indexed in Pubmed: 23298207.
22. Miller D, Motomura K, Galaz J, et al. Cellular immune responses in the pathophysiology of preeclampsia. J Leukoc Biol. 2022; 111(1): 237–260, doi: 10.1002/JLB.5RU1120-787RR, indexed in Pubmed: 33847419.
23. Yang SW, Cho EH, Choi SoY, et al. DC-SIGN expression in Hofbauer cells may play an important role in immune tolerance in fetal chorionic villi during the development of preeclampsia. J Reprod Immunol. 2017; 124: 30–37, doi: 10.1016/j.jri.2017.09.012, indexed in Pubmed: 29049918.
24. Milosevic-Stevanovic J, Krstic M, Radovic-Janosevic D, et al. Number of decidual natural killer cells & macrophages in pre-eclampsia. Indian J Med Res. 2016; 144(6): 823–830, doi: 10.4103/ijmr.IJMR_776_15, indexed in Pubmed: 28474619.
25. Nakao S, Noda K, Zandi S, et al. VAP-1-mediated M2 macrophage infiltration underlies IL-1β- but not VEGF-A-induced lymph- and angiogenesis. Am J Pathol. 2011; 178(4): 1913–1921, doi: 10.1016/j.ajpath.2011.01.011, indexed in Pubmed: 21435467.
26. Ito Y, Matsuoka K, Uesato T, et al. Increased expression of perforin, granzyme B, and C5b-9 in villitis of unknown etiology. Placenta. 2015; 36(5): 531–537, doi: 10.1016/j.placenta.2015.02.004, indexed in Pubmed: 25725937.
27. Bezemer RE, Schoots MH, Timmer A, et al. Altered Levels of Decidual Immune Cell Subsets in Fetal Growth Restriction, Stillbirth, and Placental Pathology. Front Immunol. 2020; 11: 1898, doi: 10.3389/fimmu.2020.01898, indexed in Pubmed: 32973787.
28. Vinnars MTN, Rindsjö E, Ghazi S, et al. The number of CD68(+) (Hofbauer) cells is decreased in placentas with chorioamnionitis and with advancing gestational age. Pediatr Dev Pathol. 2010; 13(4): 300–304, doi: 10.2350/09-03-0632-OA.1, indexed in Pubmed: 19642814.
29. Jetten N, Verbruggen S, Gijbels MJ, et al. Anti-inflammatory M2, but not pro-inflammatory M1 macrophages promote angiogenesis in vivo. Angiogenesis. 2014; 17(1): 109–118, doi: 10.1007/s10456-013-9381-6, indexed in Pubmed: 24013945.
30. Lash GE, Pitman H, Morgan HL, et al. Decidual macrophages: key regulators of vascular remodeling in human pregnancy. J Leukoc Biol. 2016; 100(2): 315–325, doi: 10.1189/jlb.1A0815-351R, indexed in Pubmed: 26819320.
31. Liu X, Fei H, Yang C, et al. Trophoblast-Derived Extracellular Vesicles Promote Preeclampsia by Regulating Macrophage Polarization. Hypertension. 2022; 79(10): 2274–2287, doi: 10.1161/HYPERTENSIONAHA.122.19244, indexed in Pubmed: 35993233.